Supplementary Information

2-Aza-1,3-butadiene ligands for the selective detection of Hg^{2+} and Cu^{2+} ions

Rosario Martínez, Fabiola Zapata, Antonio Caballero, Arturo Espinosa, Alberto Tárraga*, and Pedro Molina*

Departamento de Química Orgánica. Facultad de Química. Universidad de Murcia. Campus de Espinardo, 30071 Murcia. Spain
E-mail: atarraga@um.es; pmolina@um.es

Dedicated to Professor Benito Alcaide on the occasion of his 60th anniversary

Contents

Figure SI 1: Cyclic voltammogram of **7** S3
Figure SI 2: Cyclic voltammogram of **9** S3
Figure SI 3: Changes in the linear sweep voltammogram of **7** upon addition of increasing amounts of Cu^{2+} cations and Hg^{2+} cations. S4
Figure SI 4: Changes in the linear sweep voltammogram of **9** upon addition of increasing amounts of Cu^{2+} cations and Hg^{2+} cations. S4
Figure SI 5: Evolution of the DPV of **6** upon addition of increasing amounts of Zn^{2+} cations. S5
Figure SI 6: Changes in the absorption spectra of **6** and **7** in CH_3CN upon addition of increasing amounts of Hg^{2}. S5
Figure SI 7: Fluorescence emission spectra of ligands **6** and **8** in CH_3CN upon titration with Hg^{2}. S6
Figure SI 8: Evolution of the fluorescence emission spectra of **8** in CH_3CN upon addition of increasing amounts of Zn^{2+} S6
Figure SI 9: Evolution of the UV/visible spectra of **10** in CH_3CN upon addition of increasing amounts of Cu^{2+} and Hg^{2+} S7
Figure SI 10: Evolution of the fluorescence emission spectra of **10** in CH_3CN upon addition of increasing amounts of Cu^{2+} and Hg^{2+} S7
Figure SI 11: Job's plot for **7** and **9** with Hg^{2+} S8
Figure SI 12: Job's plot for **10** and Cu^{2+} S8
Figure SI 13: Stepwise complexation/descomplexation cycles of ligands **7** and **9** with Hg^{2+} S9
Figure SI 14: Stepwise complexation/descomplexation cycles of

ligand **10** and Cu^{2+} S9
Figure SI 15. Plot for determining the detection limit of **6** towards Hg^{2+} S10
Figure SI 16. Plot for determining the detection limit of **7** towards Hg^{2+} S10
Figure SI 17. Plot for determining the detection limit of **8** towards Hg^{2+} S11
Figure SI 18. Plot for determining the detection limit of **8** towards Zn^{2+} S11
Figure SI 19. Plot for determining the detection limit of **9** towards Hg^{2+} S12
Figure SI 20. Plot for determining the detection limit of **10** towards Hg^{2+} S12
Figure SI 21. Plot for determining the detection limit of 10 towards Cu^{2+} S13
Calculated structures: cartesian coordinates and energies S14

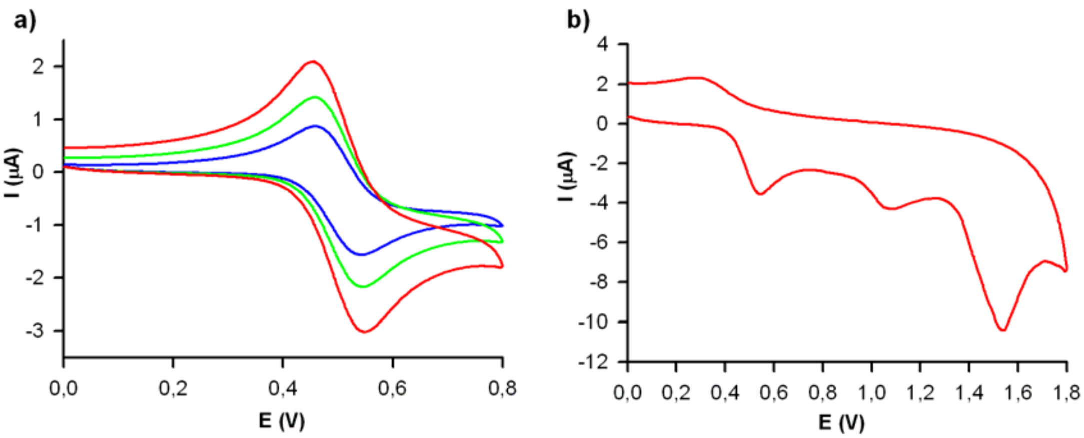

Figure SI 1: Cyclic coltammogram of **7** in CH_3CN using n-Bu_4NPF_6 0,1 M as the supporting electrolyte, AgCl/Ag as the reference electrode, and platinum wires as the counter and working electrodes, in the presence of DMFc as the internal standard. a) Different scanning rates were used to check the reversibility of the system: (blue) 0.10 V s^{-1}, (green) 0.30 V s^{-1}, (red) 0.5 V s^{-1}. b) 0.50 V s^{-1}.

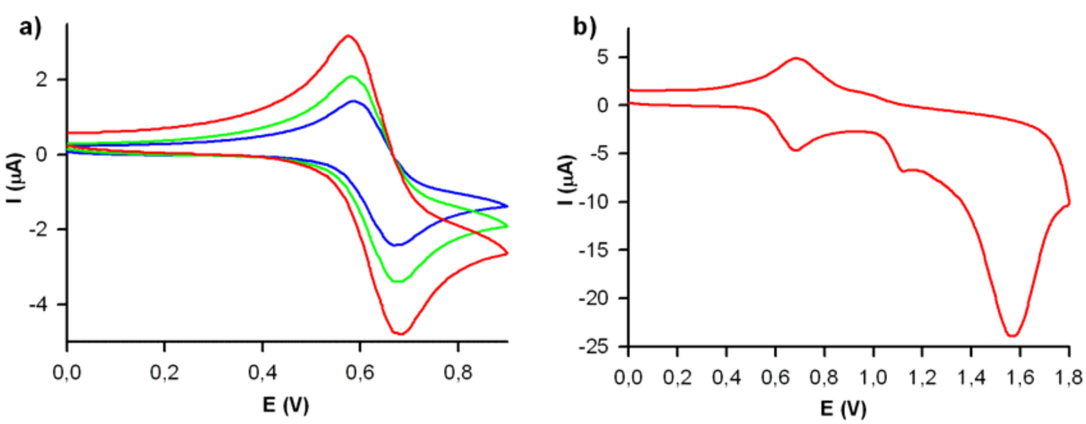

Figure SI 2: Cyclic coltammogram of **9** in CH_3CN using n-Bu_4NPF_6 0,1 M as the supporting electrolyte, AgCl/Ag as the reference electrode, and platinum wires as the counter and working electrodes, in the presence of DMFc as the internal standard. a) Different scanning rates were used to check the reversibility of the system: (blue) 0.10 V s^{-1}, (green) 0.30 V s^{-1}, (red) 0.5 V s^{-1}. b) 0.50 V s^{-1}.

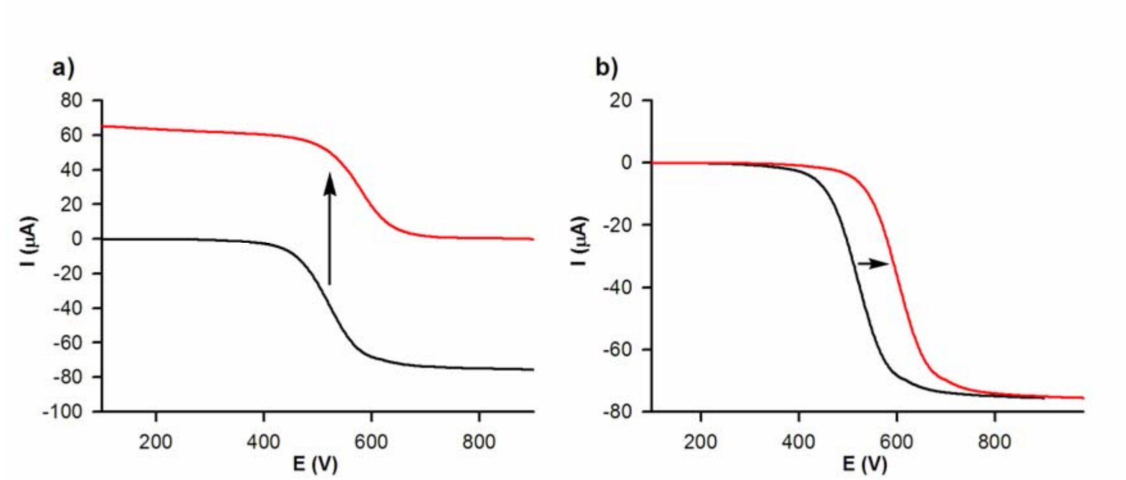

Figure SI 3: Changes in the linear sweep voltammogram of **7** (1 x 10^{-3} M) in CH_3CN with TBAP (0.1 M) as supporting electrolyte, obtained using a rotating disk electrode at 100 mV s^{-1} and 1000 rpm, when metal cations are added: (a) upon addition of increasing amounts of Cu^{2+} cations and (b) upon addition of increasing amount of Hg^{2+} cations.

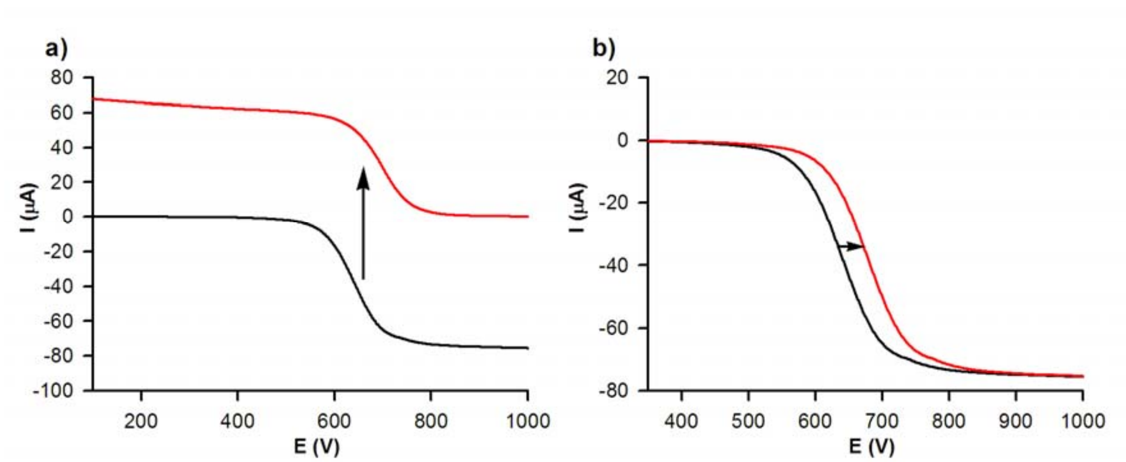

Figure SI 4: Changes in the linear sweep voltammogram of **9** (1 x 10^{-3} M) in CH_3CN with TBAP (0.1 M) as supporting electrolyte, obtained using a rotating disk electrode at 100 mV s^{-1} and 1000 rpm, when metal cations are added: (a) upon addition of increasing amounts of Cu^{2+} cations and (b) upon addition of increasing amount of Hg^{2+} cations.

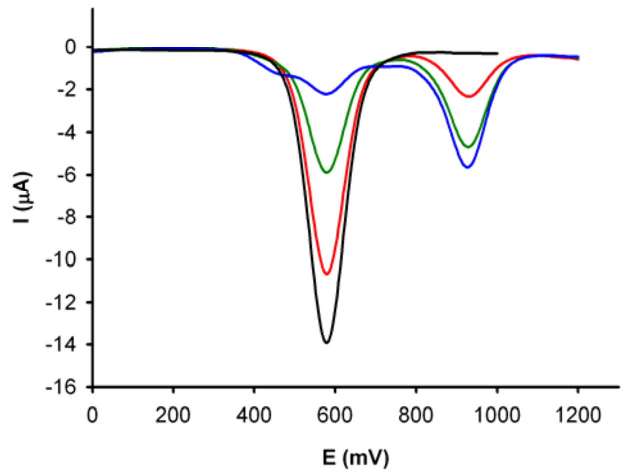

Figure SI 5: Evolution of the DPV of **6** (1×10^{-3} M) in CH_3CN with TBAP (0.1 M) as supporting electrolyte scanned at 0.1 $V.s^{-1}$ from -0 to 1.2 V when $Hg(ClO_4)_2$ is added: from 0 (black line) to 1 equiv (blue line).

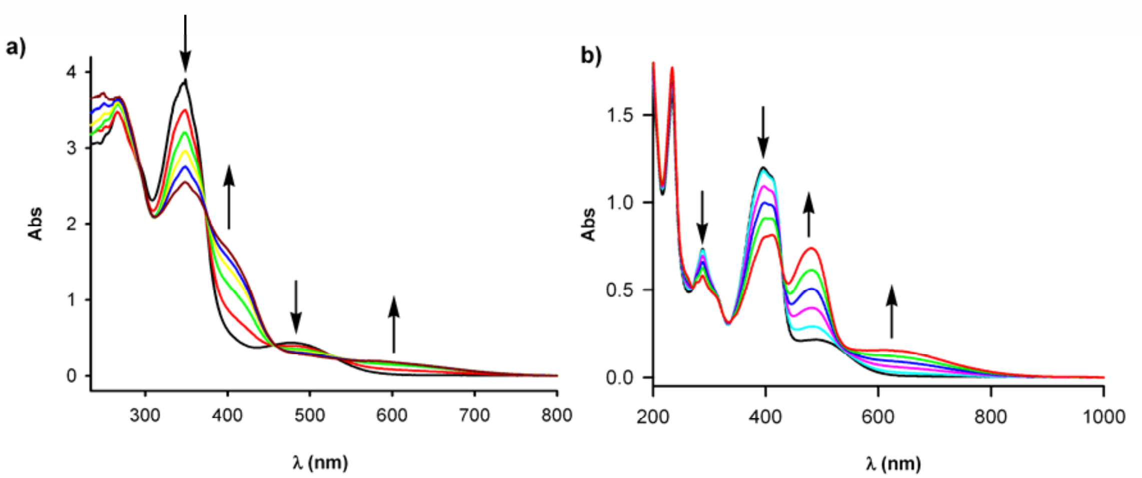

Figure SI 6: Changes in the absorption spectra of **6** a) and **7** b) (1×10^{-4} M) in CH_3CN upon addition of increasing amounts of Hg^{2+} (2.5×10^{-2} M) in CH_3CN. Arrows indicate the absorption that increase or decrease during the experiment.

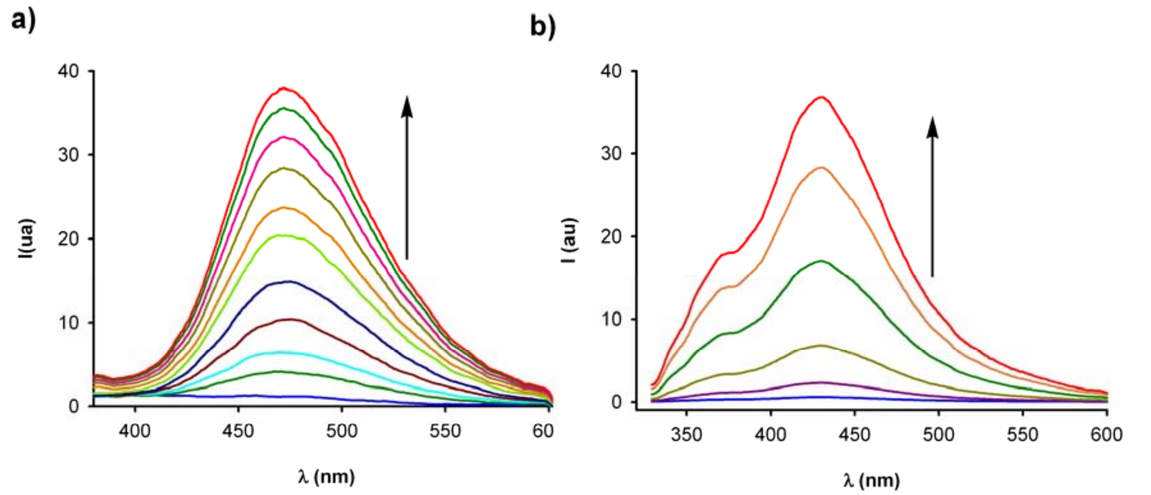

Figure SI 7: Fluorescence emission spectra of ligands **6** (a) and **8** (b) in CH_3CN ($c = 2.5x10^{-5}$ M, λ_{exc} = 310 nm) upon titration with Hg^{2+}. The initial spectra (blue) correspond to the free ligands **6** or **8** and the final spectra (red) correspond to the complexed forms **6**·Hg^{2+} and **8**·Hg^{2+} after addition of 1 equiv of Hg^{2+}.

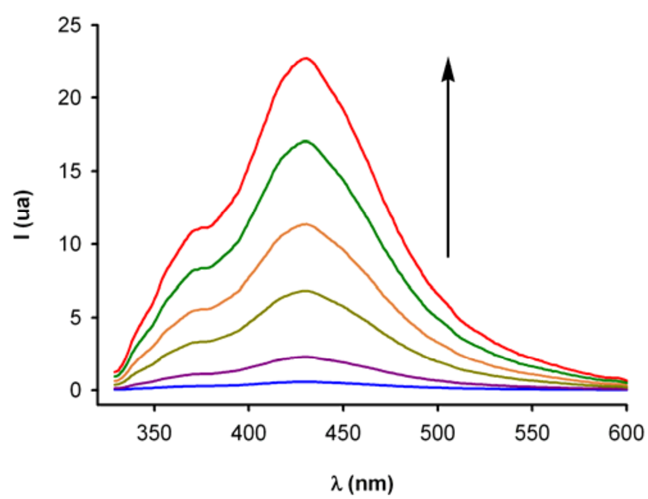

Figure SI 8: Fluorescence emission spectra of ligands **8** in CH_3CN ($c = 2.5x10^{-5}$ M, λ_{exc} = 310 nm) upon titration with Zn^{2+}. The initial spectra (blue) correspond to the free ligands **8** and the final spectra (red) correspond to the complexed forms **8**·Zn^{2+}.

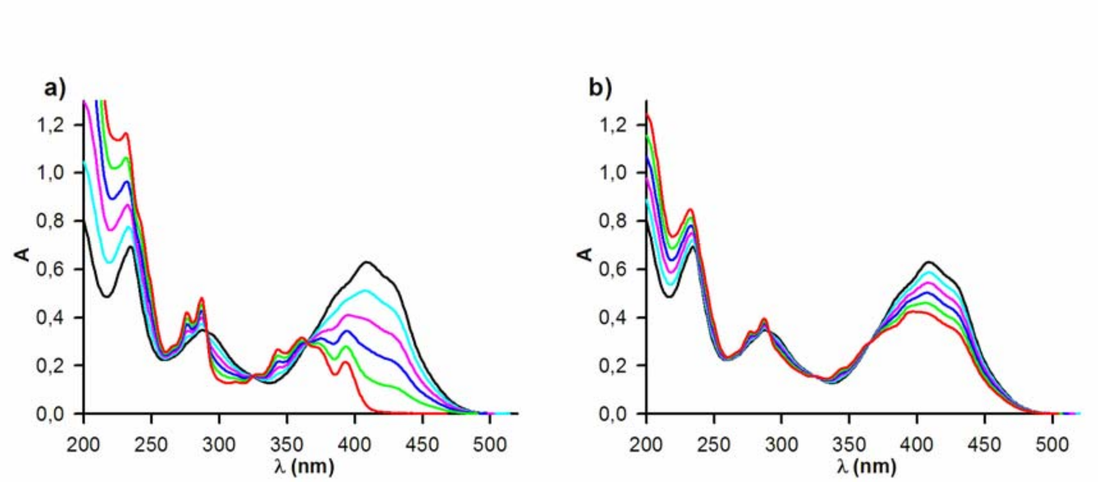

Figure SI 9: UV/visible spectra obtained during the titration of **10** in CH_3CN (c = 2.5x10^{-5} M) with Cu^{2+} (a) and Hg^{2+} (b). The initial spectra (black) correspond to the free ligand **10** and the final spectra (red) correspond to the complexed forms **10**·Cu^{2+} and **10**·Hg^{2+} after addition of 1 equiv of Cu^{2+} or Hg^{2+} respectively.

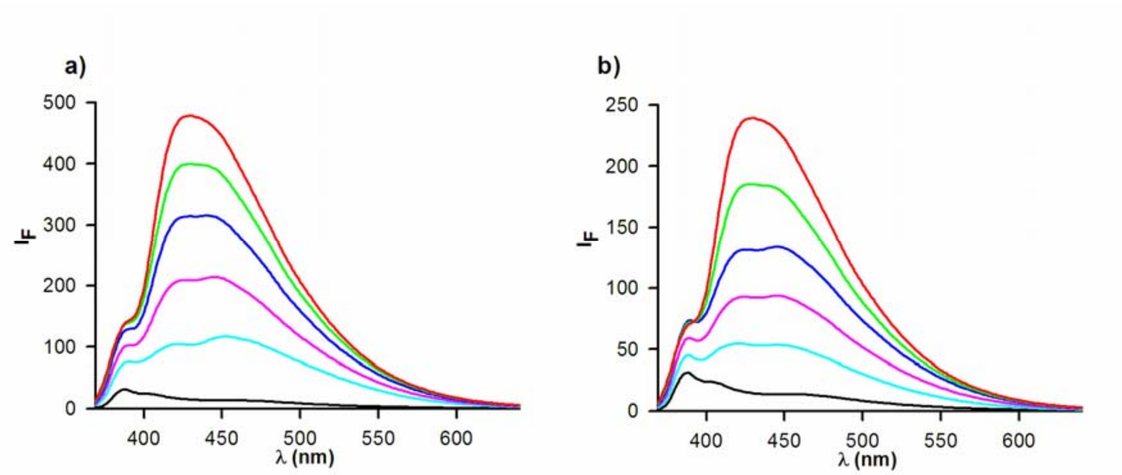

Figure SI 10: Fluorescence emission spectra obtained during the titration of **10** in CH_3CN (c = 2.5x10^{-5} M, λ_{exc} = 350 nm)) with Cu^{2+} (a) and Hg^{2+} (b). The initial spectra (black) correspond to the free ligand **10** and the final spectra (red) correspond to the complexed forms **10**·Cu^{2+} and **10**·Hg^{2+} after addition of 1 equiv of Cu^{2+} or Hg^{2+} respectively.

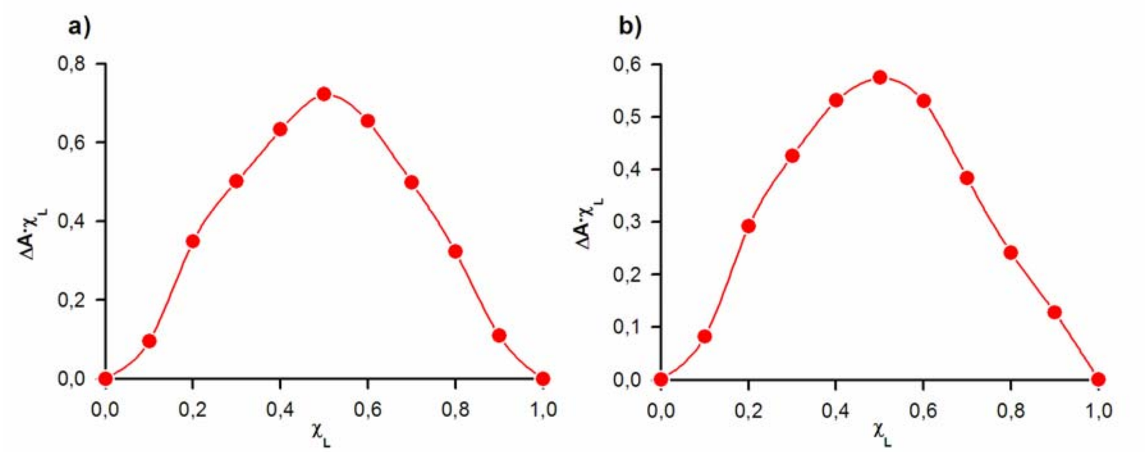

Figure SI 11: Job's plot for **7** (a) and **9** (b) titrated with Hg^{2+} indicating the formation of 1:1 complexes. The total [**L**] + [Hg^{2+}] = 1 x10^{-4} M, illustrating the 1:1 stoichiometry of the complexed formed

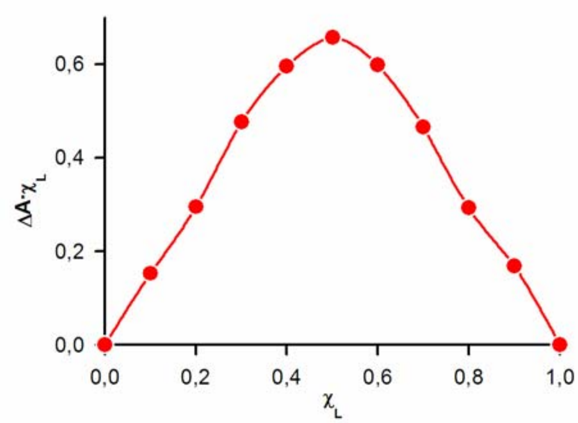

Figure SI 12: Job's plot for **10** and Cu^{2+} indicating the formation of 1:1 complexes. The total [**10**] + [Cu^{2+}] = 1 x10^{-4} M, illustrating the 1:1 stoichiometry of the complexed formed.

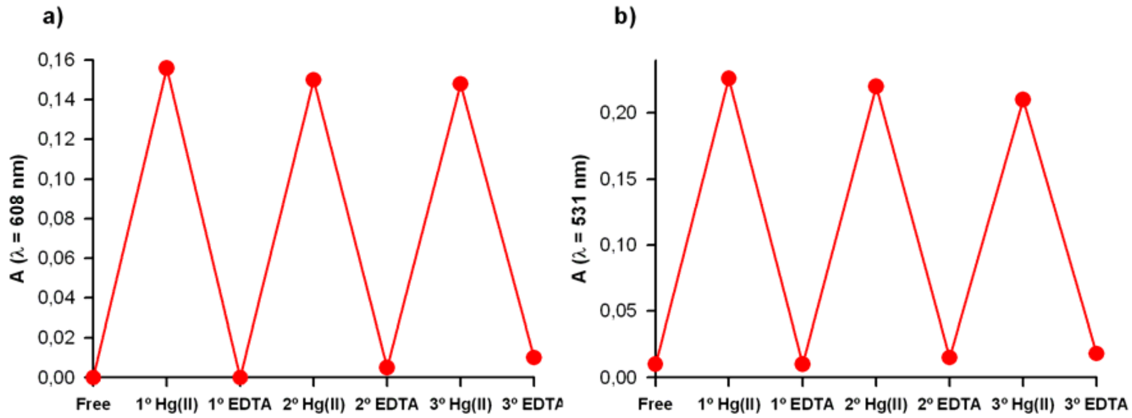

Figure SI 13: Stepwise complexation/descomplexation cycles of ligands **7** (a) and **9** (b) ($2.5 \cdot 10^{-5}$ M in CH_3CN) and Cu^{2+}, using EDTA as descomplexation agent; carried out by UV-Vis analysis.

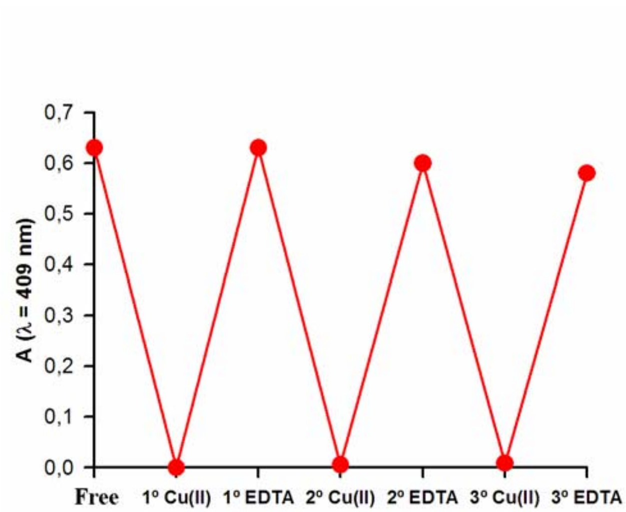

Figure SI 14: Stepwise complexation/descomplexation cycles of ligand **10** ($2.5 \cdot 10^{-5}$ M in CH_3CN) and Cu^{2+}, using EDTA as descomplexation agent; carried out by UV-Vis analysis.

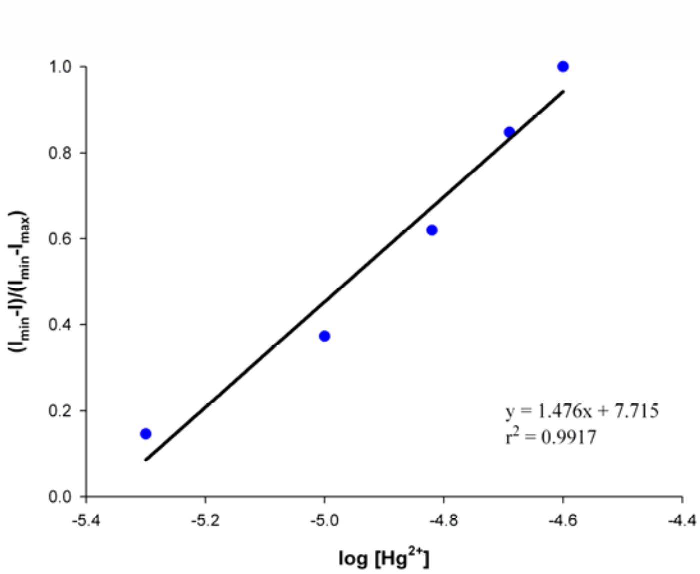

Figure SI 15. Plot for determining the detection limit of **6** towards Hg^{2+}.

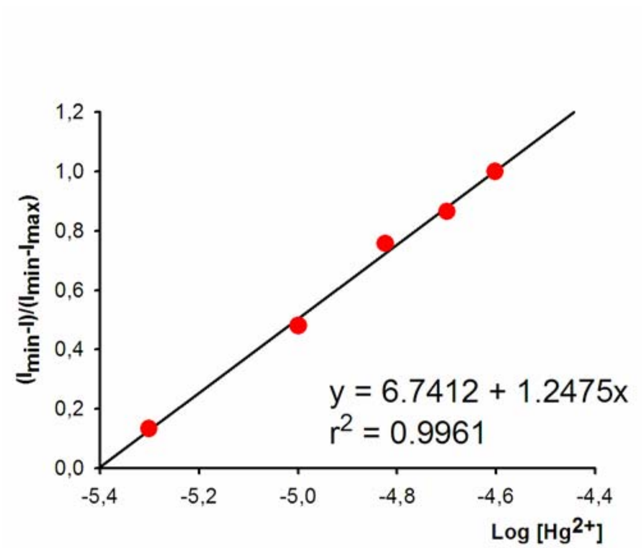

Figure SI 16. Plot for determining the detection limit of **7** towards Hg^{2+}.

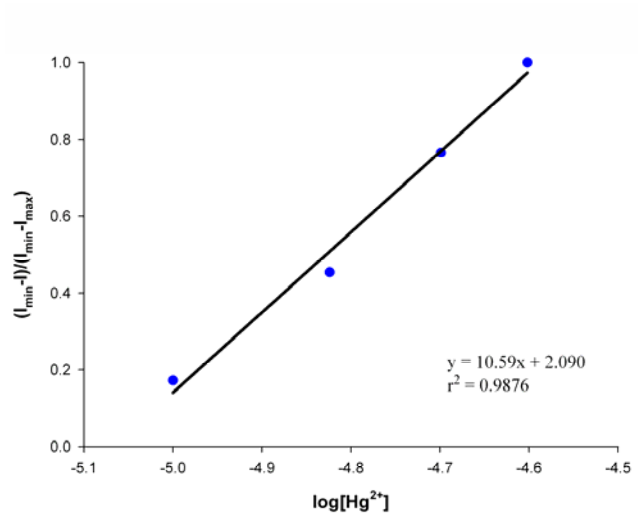

Figure SI 17. Plot for determining the detection limit of **8** towards Hg^{2+}.

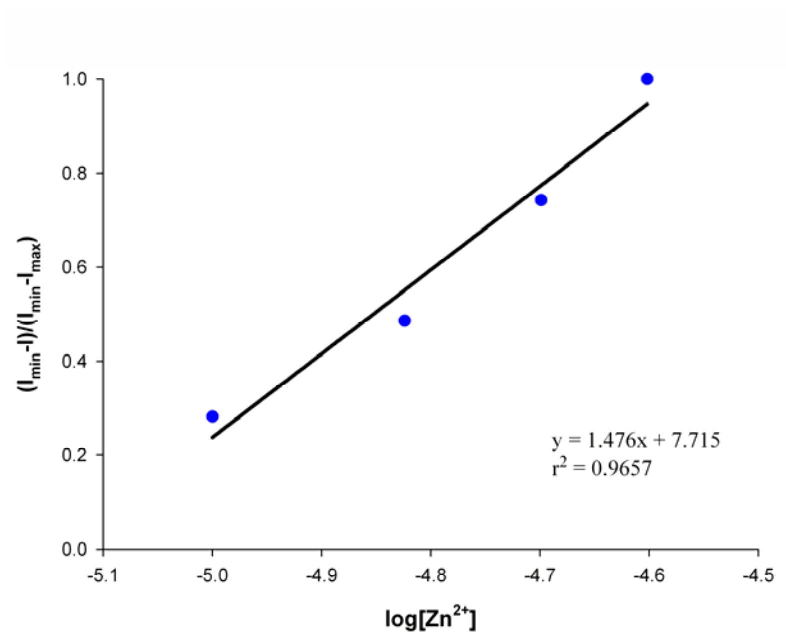

Figure SI 18. Plot for determining the detection limit of **8** towards Zn^{2+}.

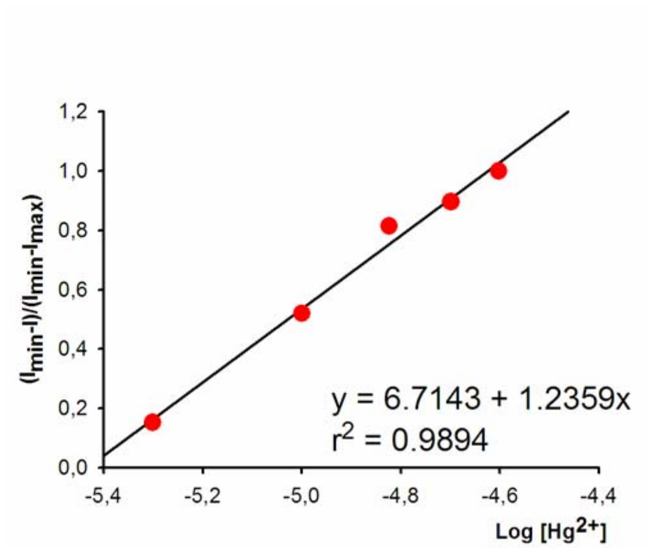

Figure SI 19. Plot for determining the detection limit of **9** towards Hg^{2+}.

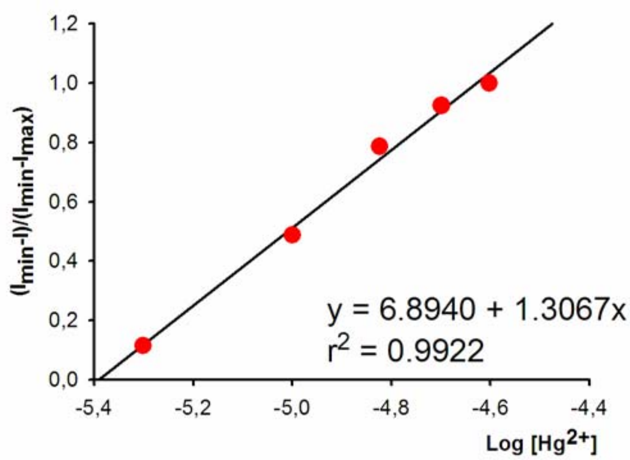

Figure SI 20. Plot for determining the detection limit of **10** towards Hg^{2+}.

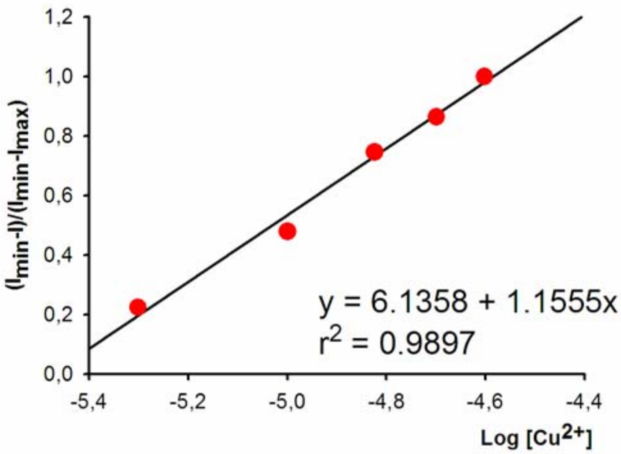

Figure SI 21. Plot for determining the detection limit of **10** towards Cu^{2+}.

Calculated structures: cartesian coordinates (in Å) and energies (au) computed for $Hg(OTf)_2$, compound **6** and complex **6**·$Hg(OTf)_2$.-

$Hg(OTf)_2$ (C_i): E_{MeCN} = -2076.368870 au

$E_{gas\text{-}phase}$ = -2076.353567 au

```
Hg  0.00000000  0.00000000  0.00000000
O   2.12336930  0.00000000  0.00000000
S   2.57798908  1.52826093  0.00000000
O   3.61124187  1.80477361  0.99035298
O   1.33621710  2.35048323 -0.08311408
C   3.39468823  1.62643249 -1.72124526
F   2.48998017  1.26891567 -2.65252958
F   3.79281088  2.88428995 -1.94444294
F   4.44442770  0.80064508 -1.77610467
O  -3.61124186 -1.80477361 -0.99035298
S  -2.57798908 -1.52826093  0.00000000
O  -2.12336930 -0.00000000  0.00000000
O  -1.33621709 -2.35048324  0.08311408
C  -3.39468823 -1.62643249  1.72124526
F  -3.79281088 -2.88428995  1.94444294
F  -2.48998017 -1.26891567  2.65252958
F  -4.44442770 -0.80064509  1.77610467
```

Compound **6**: E_{MeCN} = -2206.548381 au

$E_{gas\text{-}phase}$ = -2206.551698 au

```
C   0.00000000  0.00000000  0.00000000
N   1.29812265  0.00000000  0.00000000
C   1.95150150  1.21243241  0.00000000
C   3.30980271  1.28160877  0.00729567
H  -0.56680079  0.95253203 -0.00216619
H   1.34627761  2.13456360  0.00225608
H   3.85565129  0.33567389  0.03387862
C  -0.79760149 -1.21876295  0.00306461
C  -2.22009691 -1.11690437  0.00430153
C  -3.01106638 -2.24245882  0.00733623
C  -2.43265756 -3.54106904  0.00897543
C  -3.21630793 -4.72369392  0.01189239
C  -2.61895808 -5.96838884  0.01321114
C  -1.20681999 -6.08452103  0.01188949
C  -0.41575010 -4.95539528  0.00927346
C  -0.99763281 -3.65619133  0.00766162
C  -0.21138405 -2.48257652  0.00481083
H  -2.67593841 -0.12470351  0.00328664
H  -4.09886369 -2.15303590  0.00857150
H  -4.30402281 -4.63223298  0.01303555
H  -3.23353681 -6.86901454  0.01545446
H  -0.74794955 -7.07356936  0.01317830
H   0.67224845 -5.03944611  0.00863361
H   0.87721481 -2.55393323  0.00431020
C   4.09145769  2.49846567  0.00569071
C   5.52015258  2.56506605  0.21732045
C   5.93185220  3.93069741  0.13181230
```

```
C   4.77415727  4.72422704 -0.15506386
C   3.64612835  3.84969870 -0.24686737
H   6.16351499  1.71107258  0.41057168
H   6.94849069  4.29860084  0.23471334
H   4.76062371  5.79894673 -0.31164009
H   2.62985442  4.14925060 -0.48512989
Fe  5.06082244  3.32536365 -1.60645489
C   5.23749544  1.94396513 -3.09952990
C   4.16336843  2.85177631 -3.37399509
C   4.70715212  4.17648336 -3.42527395
C   6.11584154  4.08670866 -3.18018742
C   6.44312675  2.70688760 -2.97782818
H   5.14448911  0.86958459 -2.97155823
H   3.11772463  2.58334139 -3.49172864
H   4.14582555  5.09130984 -3.59082486
H   6.80866409  4.92127772 -3.12632899
H   7.42743575  2.31229702 -2.74387540
```

Complex **6·Hg(OTf)₂** :

E_{MeCN} = -4282.936560 au

$E_{gas\text{-}phase}$ = -4282.956350 au

E_{BSSE} = 0.009039 au

```
C   0.00000000  0.00000000  0.00000000
N   1.31295672  0.00000000  0.00000000
C   2.04675633  1.17592117  0.00000000
C   3.39627782  1.19120879  0.17743498
H  -0.51202544  0.96600354  0.10132742
H   1.47525286  2.09904591 -0.13763368
H   3.91673443  0.24470441  0.34898930
C  -0.80571845 -1.20231111 -0.06931491
C  -2.04459161 -1.25246536  0.63880725
C  -2.79073604 -2.40749171  0.65590526
C  -2.36918732 -3.57280990 -0.04459401
C  -3.11803078 -4.77583431 -0.03980191
C  -2.68564369 -5.87385204 -0.75816215
C  -1.48962448 -5.81523834 -1.51385811
C  -0.73568399 -4.66010241 -1.54340513
C  -1.15098953 -3.51835016 -0.80545656
C  -0.40142289 -2.31601400 -0.81115243
H  -2.37426070 -0.37510609  1.19657155
H  -3.72465212 -2.44522534  1.21882743
H  -4.04140479 -4.82048164  0.53956972
H  -3.26793840 -6.79532337 -0.74507233
H  -1.16165652 -6.69247934 -2.07114268
H   0.19713435 -4.60814549 -2.10633741
H   0.44010096 -2.25025497 -1.50610422
C   4.22369539  2.36701559  0.19725357
C   5.62012991  2.36482548  0.58299751
C   6.13234630  3.68459220  0.40738901
C   5.08295310  4.50787795 -0.11484609
C   3.91053046  3.70338982 -0.26003757
H   6.16172880  1.50037903  0.95604512
H   7.15241786  4.00105586  0.60269091
H   5.17184276  5.55530277 -0.38719884
H   2.95692393  4.03775781 -0.65814400
Fe  5.43137415  2.92468996 -1.35326818
C   5.51604737  1.41612978 -2.74615689
```

C	4.74702445	2.52340401	-3.23295474
C	5.59003874	3.68222783	-3.23769403
C	6.87762174	3.29136881	-2.74564108
C	6.82883717	1.89203614	-2.44239015
H	5.14704827	0.40707180	-2.58191592
H	3.70482330	2.48970916	-3.53587486
H	5.29892849	4.68498584	-3.53608995
H	7.73151710	3.94660546	-2.60166295
H	7.63778784	1.30068394	-2.02431070
Hg	2.40560869	-1.98861340	0.14548307
O	2.72032435	-3.52629805	1.80314963
S	3.92014367	-2.92970610	2.57575384
O	4.93377619	-3.89596805	2.99502572
O	4.34693522	-1.66462093	1.88219741
C	3.07526884	-2.31387571	4.16297880
F	3.96424060	-1.67974428	4.94705414
F	2.08744762	-1.44511707	3.83679271
F	2.54005007	-3.33953548	4.84467224
O	2.54067908	-3.47210335	-1.78476257
S	3.71247415	-2.78842503	-2.48899340
O	4.10162733	-1.56691035	-1.67646593
O	3.59737135	-2.62647415	-3.94099168
C	5.15437008	-3.99258272	-2.19660531
F	4.89401882	-5.17501581	-2.78120802
F	6.28436290	-3.48281058	-2.72118484
F	5.33037710	-4.18263737	-0.875651